Characteristic x rays from multiple-electron capture by slow highly charged Ta^{q+} ions from He and Xe atoms

S. Madzunkov,[1,2] D. Fry,[2,†] E. Lindroth,[1] and R. Schuch[1,*]
[1]*Department of Atomic Physics, Stockholm University, Alba Nova S-10691 Stockholm, Sweden*
[2]*Department of Physics, Kansas State University, Manhattan, Kansas 66506, USA*
(Received 22 January 2004; revised manuscript received 11 October 2004; published 16 March 2006)

Characteristic x rays, emitted by slow (velocity $v \sim 0.3$ a.u.) highly charged Ta^{q+} ($q=41-49$) ions after multiple capture from He or Xe atoms, were investigated in coincidence with recoil ions. The x-ray spectra are distinctly different for single and double capture as well as for different target ionization potentials (He and Xe). For the open M-shell configurations of the projectile ($q>45$) the spectra are dominated by cascade transitions. There is no evidence for direct radiative transitions from Rydberg states into the M shell, indicating dominant capture into angular momentum states that forbids such transitions. From such features we get, by comparison with spectra obtained from the calculation of the radiative cascades, the angular momentum values of the captured electron. A simple model, including autoionization, is used to relate double- and single-capture x-ray spectra and to explain their differences. The x-ray spectra with projectiles having no initial M vacancies ($q<45$) can have an important contribution from the internal dielectronic excitation (IDE) process. It is found that this channel is drastically reduced for double capture from He and closed for projectiles with $q=41$, as expected from our calculations of the core-excited states in $Ta^{(q-1)+}$. The x-ray spectra and photon yields in these heavy systems are thus determined by a competition between the relaxation channels: radiative relaxation, IDE, and, for multiple capture, autoionization.

DOI: 10.1103/PhysRevA.73.032715 PACS number(s): 34.70.+e, 32.30.Rj

I. INTRODUCTION

Single- and multiple-electron capture by slow highly charged ions have been investigated in great detail over the last two decades [1]. These investigations have been stimulated by an interest from areas such as astrophysics, hot plasma physics, and plasma diagnostics. Recently, there was an unexpected discovery of x rays emitted from the tail of the Hyakutake comet [2]. The x rays seem to have their origin in the collisions of solar wind highly charged ions with atoms in the comet's coma [3]. This discovery has spawned an interest in the analysis of the x rays emitted by ions after the capture process [4,5]. For a better understanding of the x-ray spectra it is important to untangle the contributions to the x-ray spectra from different capture channels: single capture, double capture, etc. This can be achieved by coincidence measurements.

Single-electron capture between slow ions and neutral atoms is the cleanest case of ion neutralization, accompanied by photon emission. The electron is captured in an excited state, usually a Rydberg state (n), of an ion. For light ions the classical over-the-barrier model (OBM) [6] is known to give an accurate prediction for the principal quantum number (n) of the state into which the electron is captured [1]. The relaxation of the electron, in the single-capture case, is generally via successive photon transitions. The selection rules of the dominating dipole transitions determine the possible relaxation path of the electron, which is highly dependent on the angular momentum of the capture state. Thus, by analysis of the x-ray spectrum obtained from relaxation of the captured electron, one can study the state-selective (n) capture and relaxation processes associated with the specific capture state. State-selective cross sections have been measured by different techniques, such as recoil-ion momentum spectroscopy [7–9] and photon emission spectroscopy [10–12]. With these methods, the state-selective cross sections are investigated for the case of low-charge projectiles ($q<10$) and thus only for electrons captured into low-lying states, $n<6$. In the case of slow highly charged ions only few measurements, sensitive to the angular momentum of the capture states, were performed [13]. In order to get a complete picture of the relaxation mechanism, the possibility of forming doubly excited states even in the single capture must be considered. If energetically possible, the captured electron can excite the ion core, leading to the formation of a doubly excited state. This mechanism, known as internal dielectronic excitation (IDE) [14], was discussed in detail by Schuch *et al.* for single-electron capture [15] and multiple-electron capture [16]. IDE becomes energetically possible first for electrons in the M shell, where it can create additional M-shell vacancies. Thus, in the case where the slow ion has initially no M vacancy it can still emit characteristic M x rays after capture of an electron into a high-n state.

A description of multiple capture is by far more complicated. It demands a solution of a time-dependent problem involving several particles. A complete time-dependant description is often too complicated to be practical. Instead, attempts have been made to describe multiple capture by a somewhat modified OBM. This extended classical over-the-barrier (ECB) model [17] describes multiple capture as the

*Electronic address: schuch@physto.se
†Present address: Polymers Division, National Institute of Standards and Technology, 100 Bureau Drive MS 8542, Gaithersburg, MD, 20899, USA.

successive transfer of electrons at critical distances. It also accounts for the possible recapture of a transferred electron. In multiple-capture cases, not only radiative relaxation and IDE, but also Auger transitions [18] must be considered. These three processes compete, and for a proper understanding of multiple-electron capture stabilization, the branching ratios of these processes should be determined.

We have thus investigated the characteristic M x rays following capture by slow Ta^{q+} ions ($q=41-49$) with targets heaving quite different ionization potentials: He and Xe. The x rays are measured in coincidence with recoil ions as described in Sec. II. This allowed us to observe x rays originating from single and multiple capture separately. This exposes the influence of autoionization on the x-ray spectra. We will present a model that relates the single-capture x-ray spectra to those from double capture (Sec. III). The projectile charge states cover two distinct regions: closed M shell ($q=41-44$) and open M shell ($q=46-49$). The influence of IDE and Auger transitions on the x-ray spectra in these two regions is discussed.

II. EXPERIMENT

The experimental setup was described in details in Ref. [16]. Here, we give only a short description. The highly charged Ta^{q+} ($q=41-49$) ions were produced in a Cryogenic electron beam ion source (CRYEBIS) [19] at the J. R. Macdonald Laboratory, accelerated to 10 keV/q, charge analyzed, and redirected towards the interaction region. The interaction region was a gas cell containing He or Xe atoms. The pressure in the gas cell was kept low enough to ensure that only single collisions take place between Ta^{q+} ions and target atoms. After passing the interaction region, Ta^{q+} ions were counted by a channeltron. In the interaction between projectile ions and a target atoms in the gas cell, x rays as well as a recoil ion can be produced. The x rays were detected by a Si(Li) detector with an acceptance angle of 0.36 sr. That is small enough so that even in the case where several x rays are produced in a single collision the chance of pileup is very small. In fact, we did not observe any indication of pileup in the measured spectra. The recoil ions were extracted by an electric field, time-of-flight (TOF) analyzed and detected by a multichannel plate detector (MCP).

Recoil ions were recorded in coincidence with both projectiles and x rays. Thus for each measurement, performed for a specific ion charge state and atom species, we obtain three entangled spectra: recoil TOF from projectile coincidence, recoil TOF from x-ray coincidence, and x-ray energy for different numbers of captured electrons, r.

The energy calibration of the Si(Li) detector was performed using known $K\alpha$ and K_β x-ray energies of Al, Ti, NaCl, SiO_2, and Mn obtained from an ^{55}Fe source. The energy resolution was determined to be 150 eV at 1.5 keV and 180 eV at 5.9 keV.

The following major experimental obstacles need to be considered. First, the Ta ions could be in metastable states. The formation of metastable states in the CRYEBIS is possible. However, the way CRYEBIS operates makes "survival" of metastable ions in the extracted beam unlikely. In order to check the existence of metastable states we checked the x-ray count rate as a function of the projectile charge state. The signature of metastable states in such a measurement would be a dramatic change in the x-ray count rate. We observed no such change, and thus we believe that no metastable ions reached the interaction region. A further point is the x-ray detection efficiency. We selected a Si(Li) detector for having optimum detection efficiency in an energy window of 1–4 keV, given by the expected M–x-ray transitions of Ta. The detector allows observation of x rays from 1 keV to 20 keV, where the lower limit is given by the absorbing components of the Si(Li) detector and the high-energy limit by the thickness of the Si(Li) detector zone [20]. Special precautions were made to be sure that x rays at around 4 keV were detected with unity efficiency. A possible loss of efficiency was checked by comparing the ratios of the "escape peaks" (arises from the escape of $K\alpha$ x rays of silicon) to the original x-ray peaks with the probability for creation of the escape peak [22]. We did not identify any abnormalities in the detector efficiency. At 1 keV the absorption correction from the 12-μm Be window, 0.2-μm Au contact, and 0.02-μm Si dead layer was a factor of 4 and the spectra were corrected accordingly. Below 1 keV the absorption correction rises sharply and one should not consider the spectra in that range.

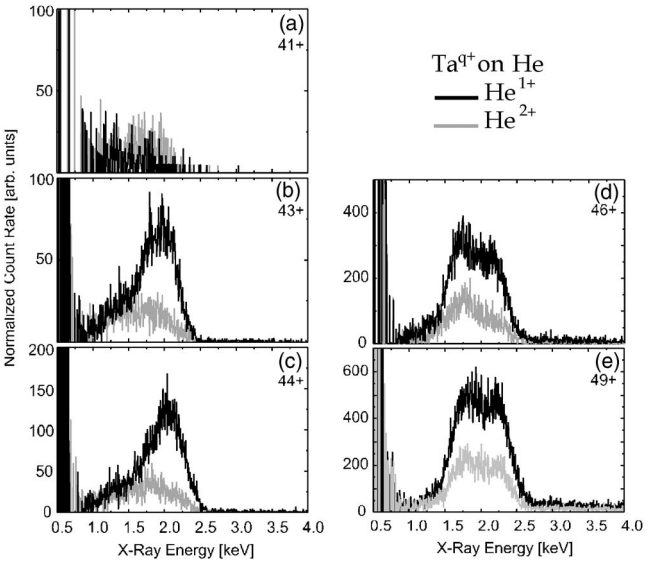

FIG. 1. X-ray spectra for single- and double-capture events in collisions of Ta^{q+} ($q=41,43,44,46,49$) with He, black line and grey line, respectively. (a), (b), and (c) ($q=41,43,44$) are for a closed M shell in the Ta core. (d) and (e) ($q=46,49$) are for an open M shell in the Ta core.

In order to compare the intensities of x-ray energy spectra recorded for different projectile charge states, we normalized them on target pressures (target densities) and projectile count rates.

III. RESULTS AND DISCUSSION

In Figs. 1 and 2 we present x-ray spectra from single- and double-capture events in collisions of Ta^{q+} ions with He at-

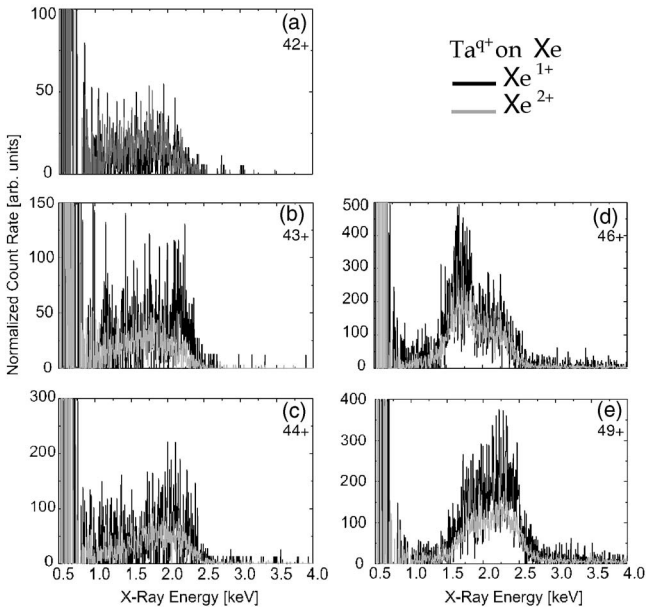

FIG. 2. X-ray spectra for single and double-capture events in collisions of Ta^{q+} (q=42,43,44,46,49) and *Xe* target, black line and grey line, respectively. Figures (a), (b), and (c) (q=42,43,44) are for closed *M* shell in *Ta* core. Figures (d) and (e) (q=46,49) are for open *M* shell in *Ta* core.

oms for q=41,43,44,46,49 and Xe atoms for q =42,43,44,46,49. Note that equal x-ray intensities (for single and double capture) do not imply equal probabilities for single and double capture, since the spectra are normalized on the number of projectiles. On the left-hand side of the figures [Figs. 1(a)–1(c) and Figs. 2(a)–2(c)] we present the x-ray spectra from capture by Ta^{q+} ions with closed *M*-shell configurations and on the right-hand side [Figs. 1(d) and 1(e) and Figs. 2(d) and 2(e)] the spectra from capture by ions with open *M*-shell configurations. Considerable differences in the spectra for these two groups can be noted.

For Ta^{41+} and Ta^{42+}, the x-ray intensities for single and double capture are approximately the same, and the intensities are almost one order of magnitude smaller than for the other charge states. For Ta^{43+} and Ta^{44+} the x-ray spectra change dramatically in the case of He atoms. The prominent peak at 2.1 keV observed in single-capture x-ray spectra does not exist in the double-capture x-ray spectra. Furthermore, aside from different intensities, there is a similarity in the spectra between single capture for q=41 and double capture for q=43 and 44. In the case of Xe [see Fig. 2(a)–2(c)], there is a clear difference in the x-ray intensities for different charge states. However, the shapes of x-ray spectra for single- and double-capture cases are similar.

Changing the projectile charge state to 46+ and 49+ (open *M* shell) the spectra again change dramatically [see Figs. 1(d) and 1(e) and Figs. 2(d) and 2(e)]. There is a clearly visible double peak. This suggests that the mechanism for the production of x rays in the open- and closed-*M*-shell regions is different. The spectra for capture from Xe are also very different from those for capture from He. In Xe, but not in He, the relative intensities between the peaks at ~1.7 keV and ~2.2 keV change significantly between q=46 and 49.

Before we continue with the discussion, we present the predictions of the ECB model as well as estimates for autoionization and IDE probabilities for our collision systems.

The ECB model [17] is used to calculate the principal quantum numbers n of states into which electrons are captured. For the narrow range of projectile charge states presented here, n varies only slightly. According to the ECB model, Ta^{45+} ions successively capture electrons into n_1 =16 and n_2=11 states from He and into n_1=23 and n_2=17 from Xe. In the double-capture case, Auger transitions are an important part of the relaxation process. Assuming a minimum energy of the ejected electron, we estimate the final states of the bound electrons after an Auger transition to be n_3=9 for He and n_3=14 for Xe. In Ref. [16], the Auger probabilities P_A after double capture into Ta^{q+} (q=41–49) from He and Xe were determined to be 0.5(2) and 0.7(2), respectively.

The relaxation mechanism and the x-ray emission after single capture were discussed by Schuch *et al.* [15]. There it was shown that IDE plays an important role in relaxation of captured electrons with an initially filled *M* shell. This process produces an *M*-shell vacancy into which an outer electron can decay and, in the case of Ta^{43+}, produces an x ray at ~2.1 keV. It was also shown by Schuch *et al.* that IDE is sensitive to the energy matching between single and doubly excited states. Since the number of bound doubly excited states increases with projectile charge state, the probability for IDE also increases. We calculated, using the methods described in Ref. [15], that for q=41 there are only a few bound doubly excited states. Consequently, the probability for IDE in q=41 case is close to zero. In Ref. [16] more details of the IDE probability as a function of the charge state can be found. In short, the IDE probability increases from ~15% to ~40% when the projectile charge state is increased from q=42 to q=44; see Ref. [15].

In the following we try to explain the differences between single and double capture, seen in Figs. 1 and 2, and their characteristics. In that discussion we consider open- and closed-*M*-shell configurations of the projectile separately.

For q=41, the IDE channel is closed and all the x rays originate from Auger and radiative cascading. The direct transition from n=15 to n=4 in Ta^{41+} is in the 1.4–1.8-keV energy range. The low count rate in this energy region [see Fig. 1(a)] indicates that only a few of the x rays in the spectrum come from direct transitions. The probability for direct transitions should be more or less the same for all closed-*M*-shell configurations of Ta^{q+} (q=41–43). Thus, by comparing the x-ray intensities for Ta^{41+} and Ta^{43+} we can estimate that only about 10% of captured electrons undergo a direct transition in Ta^{43+}. This is surprising since direct transitions, if allowed by the dipole selection rule, should be more probable than successive cascading.

For q=43 and 44, the IDE process is energetically possible [15] which explains the prominent peak at ~2.1 keV for single capture from He. However, the spectrum for double-capture case does not show this peak, which suggests that there the IDE process is insignificant. Indeed, our calculation of the Ta^{q+} (q<46) states shows virtually zero probability for the IDE process in the case of n=9 or lower capture state. This n=9 state is the highest one expected to be

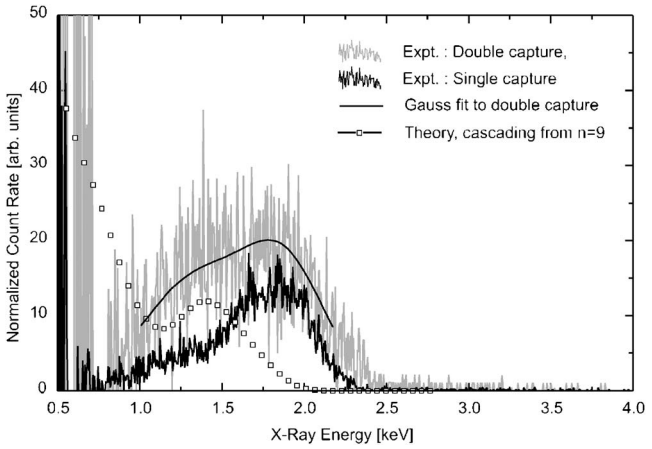

FIG. 3. X-ray spectra from single- and double-capture events with normalized intensities (see text) are presented by dark and gray wiggling lines, respectively. By the solid dark line we present the Gaussian fit to the double-capture x-ray spectra. Open squares present the synthetic x-ray spectrum for one electron cascading in the Ta^{43+} core potential from the $n=9$ state.

populated when double-electron capture is followed by an Auger transition. In order to compare the single- and double-capture spectra for Ta^{43+} (see Fig. 3), we normalized them by dividing the single-capture count rate by 4. To guide the eye, we fitted the double-capture x-ray spectrum with two Gaussians shown as a solid line in Fig. 3. The square symbols show the calculated result for cascading of one electron starting in $n=9$. One can see from the figure that the 1.7–2.2 -keV region of the double-capture x-ray spectrum (grey curve) fits rather well with the "scaled" single-capture x-ray spectrum. The spectrum, in that energy range, cannot be explained by radiative cascading (open squares in Fig. 3); it must have a contribution from the relaxation of electrons through the IDE process. Note that the probability for the IDE process is here much smaller than in the single-capture case since the Auger channel is open. The low-energy part of the spectrum (1–1.5 keV) may originate from relaxation of one electron that remains after Auger transition into $n=9$.

For Xe we can see that the single- and double-capture x-ray spectra ($q=42-44$—i.e., closed M shell) have a similar shape and intensity, in contrast to the He target results [see Figs. 2(a)–2(c)]. As mentioned earlier, the ECB model predicts that the electrons are captured from Xe into higher-energy states of the projectile than from He. As a consequence, the IDE channel can be open for capture from Xe even after autoionization to $n_3=14$. Thus x-ray emission can be expected to occur in the same final cascade steps for both capture channels. That would explain the similar shape of x-ray spectra for single and double capture from Xe contrary to capture from He.

In the case where the Ta projectile has initial M-shell vacancies, additional channels for cascading exist. We would also expect the probability for the IDE process to decrease, due to its competition with direct transitions into the M shell.

In order to discuss differences between single and double capture in the open-M-shell region, we have plotted the x-ray spectra normalized at ~1.7 keV for both targets in Fig. 4. In

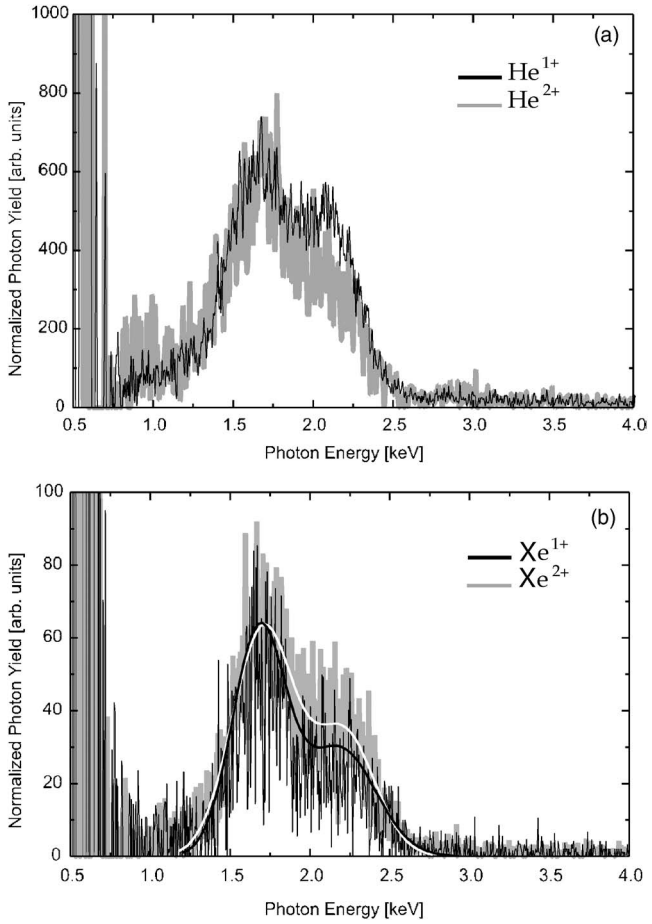

FIG. 4. X-ray spectra from Ta^{46+} single capture from He and Xe are dark wiggly lines. X-ray spectra from Ta^{46+} double capture from He and Xe are thick grey wiggly lines. Figure (b): to guide the eye, we plotted fits to the measured single and double capture spectra as solid dark and white lines, respectively.

the case of He [see Fig. 4(a)], the intensity at ~2.1 keV is clearly lower in the double-capture case. For the Xe target [see Fig. 4(b)] one cannot, within the given statistical fluctuations, recognize any difference between double and single capture. To guide the eye, we have plotted a dark and white curve representing Gaussian fits to the experimental data. The Gaussian fit indicates that single capture is, at 2.1 keV, slightly below the double capture spectrum. However, we estimate that this difference is well within the statistical uncertainty.

In the following we try to understand these features from a cascade model that invokes the features of autoionization mentioned above. We estimate [15] that the contribution to the x-ray energy spectra from IDE comes from $4f \rightarrow 3d$ transitions at ~2.1 keV. Detailed calculations of the IDE resonances are rather complicated in this case, and presently only a qualitative analysis is performed. By comparing the x-ray intensities for Ta^{44+} and Ta^{46+} [see Figs. 1(c) and 1(d) and Figs. 2(c) and 2(d)], we see that even if IDE would have the same probability in the open- and closed-M-shell regions, its contribution to the x-ray spectra in the open-M-shell region would not be more than 20%. The x-ray spectra in the case of double capture originate from two processes: one is the

simultaneous radiative stabilization of two electrons from n_1 and n_2, and the second is the relaxation of one electron from a state n_3, populated after an Auger transition. The shape of an x-ray spectrum can thus be tuned by the probability for the Auger transition (P_A). For example, if $P_A=1$, then the x-ray spectrum for double capture will be determined solely by relaxation of electrons from the state n_3. In Ref. [15], the single-capture x-ray yield $[Y_s^n(E)]$ was calculated for an electron cascading from a specific n, state in the Ta^{46+} core potential (one $3d$ hole). We followed the cascading of the electron and obtained the energy distribution of the emitted photons from the branching ratios in each step. Only dipole-allowed transitions were considered, and the energies and matrix elements were calculated within a Dirac-Fock approximation. The x-ray lines were subsequently folded with a Gaussian distribution function of a width representing the detector resolution [15]. Here we assume that the electron has equal probability to be captured into two neighboring angular momentum states ℓ^a and ℓ^b, for a specific n state. Thus, the x-ray spectrum from single capture into states with a specific n and two neighboring ℓ's is calculated as

$$Y_s^{n,\ell^{a,b}} = \frac{1}{2(\ell^a+\ell^b+1)}[(2\ell^a+1)Y_s^{n,\ell^a}(E) + (2\ell^b+1)Y_s^{n,\ell^b}(E)], \quad \ell^b=\ell^a+1. \tag{1}$$

The double-capture x-ray spectra $[Y_d^{n_1,n_2,\ell^{a,b}}(E)]$ are then calculated as

$$Y_d^{n_1,n_2,\ell^{a,b}}(E) = \frac{1}{2-P_A}\{[Y_s^{n_1,\ell^{a,b}}(E)+Y_s^{n_2,\ell^{a,b}}(E)](1-P_A) + Y_s^{n_3,\ell^{a,b}}(E)P_A\}. \tag{2}$$

Each synthetic single-capture spectrum $Y_s^n(E)$ is normalized so that the integral over the energy is equal to unity. To preserve this normalization for $Y_d(E)$, we added the normalization factor $1/(2-P_A)$ to Eq. (2). In Fig. 5 we have plotted the synthetic spectra calculated using Eq. (2) together with the measured x-ray spectra for double capture of Ta^{46+} from He and Xe. The values for neighboring ℓ's are indicated in the figure. One can see that for $=1,2$, the main contribution to the intensity comes from $n=4\rightarrow3$ transitions. The direct $(n_{1(2,3)}\rightarrow3)$ transitions as well as $n=5\rightarrow3$ transitions are, for $\ell=3,4$, clearly visible in the synthetic spectra. Note that both transitions are very weak in the measured spectra. For $\ell=5,6$ and higher, the electrons are cascading through "YRAST lines" and neither direct transition nor $4p\rightarrow3d$ transitions occur.

Of the various synthetic spectra illustrated in Fig. 5, the synthetic spectrum for $\ell=1,2$ (shown as a solid grey line) is the closest match to experimental data for both target cases. First, it does not contain the $n=5\rightarrow3$ transition nor direct transition $n_{1(2,3)}\rightarrow3$. Second, the $n=4\rightarrow3$ transition is reproduced in width as well as in shape. The largest discrepancy for the $\ell=1,2$ spectra from the measured ones occurs around 1 keV. This can partially be explained by uncertainties in the detector efficiency correction and the high statistical ($\sim20\%$) error in this energy region.

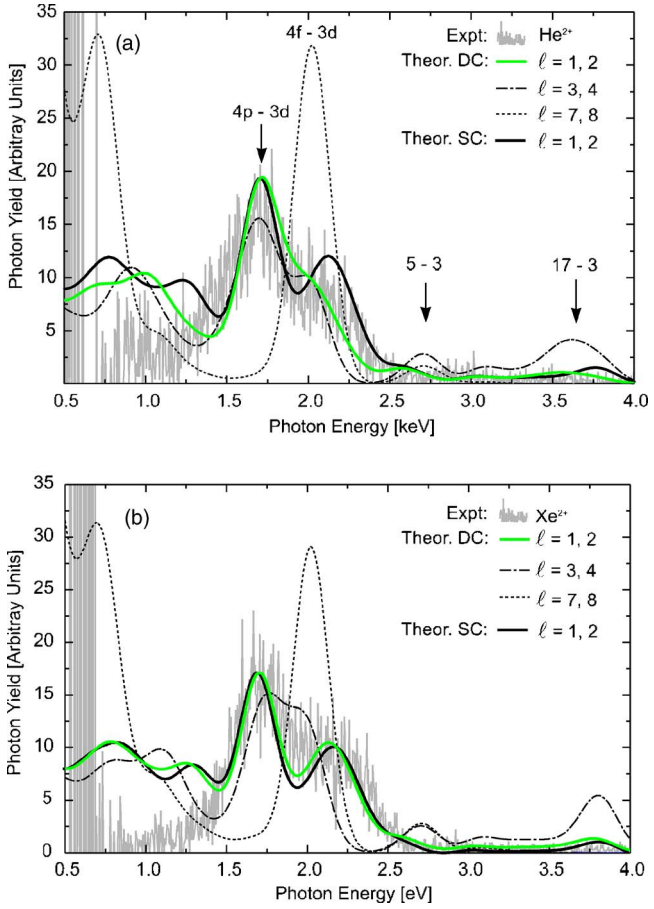

FIG. 5. (Color online) The grey wiggly lines show measured x-ray spectra for double capture. The other lines show the calculated spectra ($\ell=1,2$ etc.). The double-capture (DC) spectra are calculated using Eq. (2), and the single-capture (SC) spectrum is calculated using Eq. (1).

In Table I, we present the predictions by several models for the angular momenta of the states into which electrons are captured after single (ℓ_1) and double (ℓ_2) capture. The statistical model uses an angular momentum distribution given by $P(n,\ell)=(2\ell+1)/n^2$; i.e., for given n, the probability to capture to a specific ℓ state is weighted by its degeneracy. It is expected that this type of population occurs for higher collision velocities, where high-ℓ states are populated with larger probability. Duman *et al.* [23] represent the prob-

TABLE I. Predictions by various models for the average angular momentum populated in collisions between Ta^{46+} and He and Xe. The angular momentum of the first and second captured electrons is denoted by ℓ_1 and ℓ_2, respectively.

	He		Xe	
	ℓ_1	ℓ_2	ℓ_1	ℓ_2
Statistical model	11	7	15	11
Duman *et al.* [23]	5	5	5	5
ECB (bv, v=0.3 a.u.)	5	2	9	5
Burgdörfer *et al.* [21] (v=0.3 a.u.)	2	1	5	3

TABLE II. A comparison between measured angular momentum states and theoretical predictions of the various models for single electron capture.

	Velocity [a.u.]	Measured	Statistical model	Duman *et al.* [23]	ECB (bv)	Burgdörfer *et al.* [21]
Vernhet *et al.* [10], Al^{13+}+He	0.40	3.5	3.5	2.4	3.6	1.7
Greenwood *et al.* [12], O^{6+}+He	0.35	1.7	2.1	1.5	2.3	1
This work, Ta^{46+}+He	0.32	1–2	11	5	5	2
This work, Ta^{46+}+Xe	0.32	1–2	15	5	9	5

ability of the capture as $P(q,\ell)=(2\ell+1)/q\ \exp\{-[\ell(\ell+1)/q]\}$ (see the second row of Table I). The prediction of this model, for our collision system, is that electrons are captured into the same ℓ states from both He and Xe. In the third row of Table I, the ECB model is used to calculate the values of ℓ using the velocity of the projectile ($\mathbf{v}=0.3$ a.u.) and the distance of critical approach. According to this model, electron capture from Xe occurs at higher ℓ than from He, the reason being that the critical distance at which capture occurs is inversely proportional to the target atom ionization potential. The model developed by Burgdörfer *et al.* [21] (see fourth row of Table I), is based on the ECB model, with inclusion of the centrifugal term and the projectile velocity.

As can be seen from Table I, the predicted range of ℓ's varies significantly between the models. The model given by Burgdörfer *et al.* [21] gives the best agreement with our deduced results ($\ell=1,2$), for the capture from He targets. However, it predicts a higher angular momentum for the Xe target case.

In Table II we present a comparison of the various angular momentum models with experimental data for three collision systems with the same target and similar projectile velocities. Vernhet *et al.* [10] reported average angular momenta of single capture by observing the intensity ratios between Lyman emission lines. As seen in Table II their results for ℓ are in good agreement with the statistical and the ECB models. The value for ℓ obtained by Greenwood *et al.* [12], using the same spectroscopic technique as Vernhet *et al.* [10], showed lower values for ℓ than predicted by the statistical model and agrees best with the model by Duman *et al.* It is obvious that all presented models fail to predict the angular momenta of the states even for similar collision conditions. Also, note that in the case of highly charged projectiles, the variation between predictions of different models is highest.

In order to further illustrate the effect of the Auger transition on the double-capture x-ray spectrum, we have plotted in Fig. 5 also the synthetic single-capture x-ray spectra for $\ell=1$ and 2, represented by a thick dark line. It is normalized to the synthetic double-capture spectra at $\sim$1.7 keV. The photon yield is, in the case of double capture from He, lower at $\sim$2.2 keV than for single capture, which is due to the substantial difference between n_1, n_2, and n_3 energy levels. In the Xe case, the difference between synthetic single and double capture is small, which is expected, since the Auger transition does not change the energy of the remaining electron as drastically as in the case of He. Also note that, in both cases of He and Xe, the synthetic single-capture spectrum and double-capture spectrum for $\ell=1,2$ [see Figs. 5(a) and 5(b)] are quite similar to the case of the experimental single- and double-capture spectra shown in Figs. 4(a) and 4(b).

IV. CONCLUSION

Our results show that x-ray spectra emitted after electron capture by highly charged ions are distinctly different for the cases of single and double capture as well as for capture from He and Xe. By comparing spectra from ions having closed- ($q\leqslant 45$) and open-($q>45$) M shells, as well as from double- and single-capture events, we can approximately disentangle the three processes that govern the relaxation of the captured electrons: radiative decay, IDE, and, in the case of double capture, Auger decay. We find then that the probability for the IDE process is strongly dependent on the projectile charge state. For $q=44$ it reaches 40%, but for $q=41$ it is close to zero. We interpret this as an effect of the decreasing density of bound doubly excited states when the projectile charge state is decreased. For $q>45$, M x rays can be emitted during the radiative decay and thus the probability for IDE decreases. We conclude further that the key role of the Auger decay is to transfer the retained electron to a lower-n state before the radiative cascading starts. For double capture from He this lower-n state is then below the limit where IDE is possible. The x-ray spectra after single capture can be simulated if capture to a certain n quantum number is taken from ECB and the energies as well as the relative probabilities of the photons emitted during the cascade are calculated. The spectra after double capture can also be estimated by using a derived autoionization rate and then adding single-capture spectra. The comparison of different such synthetic spectra, generated with different assumptions about the angular momentum of the capture state, with the experiment suggests that states of $\ell=1$ and 2 are predominantly populated.

ACKNOWLEDGMENTS

We thank C. L. Cocke, E. Edgu-Fry, S. Hagmann, P. Richard, and M. Stöckli for their support of this experiment and many discussions, as well as H. Cederquist for numerous discussions. One of us (S.M.) acknowledges financial support from J. R. Macdonald Laboratory. Financial support for this work was also provided by the Swedish Research Council (VR).

[1] M. Barat and P. Roncin, J. Phys. B **25**, 2205 (1992).
[2] K. Dennerl, J. Englhauser, and J. Trümper, Science **277**, 1625 (1997).
[3] I. Häberli, M. Roman, I. Gombosi, I. Tamas De Zeeuw, Darren L. Combi, Michael R. Powell, Science **276**, 939 (1997).
[4] H. Tawara, P. Richard, U. I. Safronova, and P. C. Stancil, Phys. Rev. A **64**, 042712 (2001).
[5] H. Tawara, P. Richard, U. I. Safronova, A. A. Vasilyev, S. Hansen, and A. S. Shlyaptseva, Phys. Rev. A **65**, 042509 (2002).
[6] A. Bárány, G. Astner, H. Cederquist, H. Danared, S. Hult, P. Hvelplund, A. Johnson, H. Knudsen, L. Liljeby, and K.-G. Rensfelt, Nucl. Instrum. Methods Phys. Res. B **9**, 397 (1985).
[7] Hualin Zhang, X. Fléchard, A. Cassimi, L. Adoui, G. Cremer, F. Frémont, and D. Hennecart, Phys. Rev. A **64**, 012715 (2001).
[8] R. Ali, V. Frohne, C. L. Cocke, M. Stockli, S. Cheng, and M. L. A. Raphaelian, Phys. Rev. Lett. **69**, 2491 (1992).
[9] M. L. A. Raphaelian, M. P. Stöckli, W. Wu, and C. L. Cocke, Phys. Rev. A **51**, 1304 (1995).
[10] D. Vernhet, A. Chetioui, J. P. Rozet, C. Stephan, K. Wohrer, A. Touati, M. F. Politis, P. Bouisset, D. Hitz, and S. Dousson, J. Phys. B **21**, 3949 (1988).
[11] M. G. Suraud, R. Hoekstra, F. J. de Heer, J. J. Bonnet, and R. Morgenstern, J. Phys. B **24**, 2543 (1991).
[12] J. B. Greenwood, I. D. Williams, S. J. Smith, and A. Chutjian, Phys. Rev. A **63**, 062707 (2001).
[13] P. Beiersdorfer, R. E. Olson, G. V. Brown, H. Chen, C. L. Harris, P. A. Neill, L. Schweikhard, S. B. Utter, and K. Widmann, Phys. Rev. Lett. **85**, 5090 (2000).
[14] R. Schuch, D. Schneider, D. A. Knapp, D. DeWitt, J. McDonald, M. H. Chen, M. W. Clark, and R. E. Marrs, Phys. Rev. Lett. **70**, 1073 (1993).
[15] R. Schuch, S. Madzunkov, E. Lindroth, and D. Fry, Phys. Rev. Lett. **85**, 5559 (2000).
[16] S. Madzunkov, D. Fry, and R. Schuch, J. Phys. B **37**, 3239 (2004).
[17] A. Niehaus, J. Phys. B **19**, 2925 (1986).
[18] E. D. Emmons, A. A. Hasan, and R. Ali, Phys. Rev. A **60**, 4616 (1999).
[19] M. P. Stockli *et al.*, Rev. Sci. Instrum. **71**, 902 (2000).
[20] N. Selberg, C. Biedermann, and H. Cederquist, Phys. Rev. A **54**, 4127 (1996).
[21] J. Burgdörfer, R. Morgenstern, and A. Niehaus, J. Phys. B **19**, L507 (1986).
[22] J. L. Campbell, G. Cauchon, M.-C. Lepy, L. McDonald, J. Plagnard, P. Stemmler, W. J. Teesdale, and G. White, Nucl. Instrum. Methods Phys. Res. A **418**, 394 (1998).
[23] E. L. Duman, L. I. Men'shikov, and B. M. Smirnov, Sov. Phys. JETP **49**, 260 (1979).